

## **An integrated Artificial Intelligence and GIS spatial analyst tools for Delineation of Groundwater Potential Zones in complex terrain: Fincha Catchment, Abay Basi, Ethiopia**

Authors: Tamiru, Habtamu, Wagari, Meseret, and Tadese, Bona

Source: Air, Soil and Water Research, 15(1)

Published By: SAGE Publishing

URL: <https://doi.org/10.1177/11786221211045972>

---

The BioOne Digital Library (<https://bioone.org/>) provides worldwide distribution for more than 580 journals and eBooks from BioOne's community of over 150 nonprofit societies, research institutions, and university presses in the biological, ecological, and environmental sciences. The BioOne Digital Library encompasses the flagship aggregation BioOne Complete (<https://bioone.org/subscribe>), the BioOne Complete Archive (<https://bioone.org/archive>), and the BioOne eBooks program offerings ESA eBook Collection (<https://bioone.org/esa-ebooks>) and CSIRO Publishing BioSelect Collection (<https://bioone.org/csiro-ebooks>).


Your use of this PDF, the BioOne Digital Library, and all posted and associated content indicates your acceptance of BioOne's Terms of Use, available at [www.bioone.org/terms-of-use](http://www.bioone.org/terms-of-use).

Usage of BioOne Digital Library content is strictly limited to personal, educational, and non-commercial use. Commercial inquiries or rights and permissions requests should be directed to the individual publisher as copyright holder.

---

BioOne is an innovative nonprofit that sees sustainable scholarly publishing as an inherently collaborative enterprise connecting authors, nonprofit publishers, academic institutions, research libraries, and research funders in the common goal of maximizing access to critical research.

# An integrated Artificial Intelligence and GIS spatial analyst tools for Delineation of Groundwater Potential Zones in complex terrain: Fincha Catchment, Abay Basi, Ethiopia

Air, Soil and Water Research  
Volume 15: 1–15  
© The Author(s) 2022  
Article reuse guidelines:  
sagepub.com/journals-permissions  
DOI: 10.1177/11786221211045972  


Habtamu Tamiru , Meseret Wagari and Bona Tadese

Wollega University, Nekemte, Ethiopia.

**ABSTRACT:** In this paper, the performance of Artificial Intelligence (AI) in Geospatial analysis and GIS platforms for the prospecting of potential groundwater zones was evaluated in Fincha catchment, Abay, Ethiopia. Components of geospatial data under morphometric, hydrologic, permeability, and surface dynamic change were confirmed as the criteria for prospecting groundwater potential zones. The influence of the individual criterion was ranked and weighted in Artificial Neural Networks (ANN) training model and Analytical Hierarchy Process (AHP). The correctness of the weights fixed in the ANN and AHP was evaluated with target data assigned to the networks and consistency index (CI) respectively. The weighted overlay analysis in the GIS environment was implemented to generate the promising zones in both approaches (ANN and GIS). The results obtained in the ANN model and GIS were evaluated based on pumping rate and ground-truthing points. Groundwater potential zones of five and four classes were delineated in AI and GIS techniques respectively, and this is an indicator for the effectiveness of AI in geospatial analysis for prospecting of potential zones than the traditional GIS technique. The percentage of accuracy in both methods was measured from the ROC curve and AUC. Therefore, it was found that the delineated groundwater potential zones and the ground-truthing points were agreed with 96% and 91% in the AI and GIS platforms respectively. Finally, it is concluded that the ANN model is an effective tool for the delineation of groundwater prospective zones.

**KEYWORDS:** AHP, ANN model, delineation, GIS technique, groundwater prospecting

**TYPE:** Advances in Spatial Modeling, Geostatistics, and Machine Learning in Soil Science - Original Research

**CORRESPONDING AUTHOR:** Habtamu Tamiru, Department of Water Resources and Irrigation Engineering, Wollega University, Nekemte, Ethiopia.  
Email: habtemodel1345@gmail.com

## Introduction

In the olden days, people harvested and collected water from natural surface water sources (streams, rivers, and lakes), and groundwater (springs) (Li, 2016; Worqlul et al., 2017). The quantity was the primary criterion and there was no knowledge about the quality of water (Hamed et al., 2018; Ouma et al., 2020). Gradually, the number of populations increased and the level of interest of human beings become advanced (Sarkar & Mondal, 2020). To get a reliable source of water, scholars of spatial analysis and water resources development have been searching for effective tools and approaches (Sun et al., 2019). Geographic Information Systems (GIS) has played a significant role in prospecting water sources; particularly groundwater sources (Natarajan & Radhakrishnan, 2020; Rajaveni et al., 2017). The idea of applying Artificial Intelligence (AI) in different fields of spatial science was emerged to improve the accuracy of prediction, and locations in geospatial analysis (Rezaeianzadeh et al., 2014). The science of geospatial analysis plays an important role in many scientific types of research as it primarily focuses on the understanding, analyzing, and visualization of the real world based on their locations (Mandal et al., 2018). Geospatial artificial intelligence (GeoAI) is a developing principle that combines the novelties in artificial intelligence with geospatial analysis (Lohani et al., 2012). The traditional technique of spatial analysis such as Geographic Information Systems (GIS) was intensively used in many water resources. The accuracy of the predicted spatial results is evaluated by a few points obtained from the ground survey. The importance of geospatial artificial intelligence (GeoAI) is to

improve the quality and accuracy of spatial analysis that couldn't be captured in the traditional GIS technique of geospatial analysis (Thiemig et al., 2013). Surface water sources can only be utilized if the topography where the community is living and the source of water are easily linked, financially affordable to treat the water, and the source is available. Groundwater is an alternative source of drinking water and requires fewer treatment facilities and costs (Pasalari et al., 2019). If there are no sufficient skilled human power and financial support to conduct direct field-based groundwater investigation, the application of effective tools such as GIS is the best solution. However, the effectiveness of the traditional GIS technique is limited to the small spatial extent due to its dependency on the availability of data (Gedam & Dagalo, 2020). The current study attempts to expose the capacity of Artificial Intelligence (AI) in geospatial analysis to the world's community with limited data, but better accuracy in predicting the promising groundwater potential zones. To delineate potential groundwater zones; direct and indirect methods such as areal method, surface method, subsurface method, and esoteric method are intensively used in different parts of the world (Das & Pardeshi, 2018). However, the application of Artificial Intelligence (AI) in geospatial analysis and GIS in prospecting groundwater potential zones is an indirect method, in which field-based data such as resistivities and the electrical potential of the soil layers are not included. The integration of surface and subsurface methods are the best and appropriate methods in which different geophysical factors are used to determine the subsurface phenomena. The application of GIS and remote sensing for



Creative Commons Non Commercial CC BY-NC: This article is distributed under the terms of the Creative Commons Attribution-NonCommercial 4.0 License (<https://creativecommons.org/licenses/by-nc/4.0/>) which permits non-commercial use, reproduction and distribution of the work without further permission provided the original work is attributed as specified on the SAGE and Open Access pages (<https://us.sagepub.com/en-us/nam/open-access-at-sage>).  
Downloaded From: <https://complete.bioone.org/journals/Air,-Soil-and-Water-Research> on 15 Jul 2025  
Terms of Use: <https://complete.bioone.org/terms-of-use>

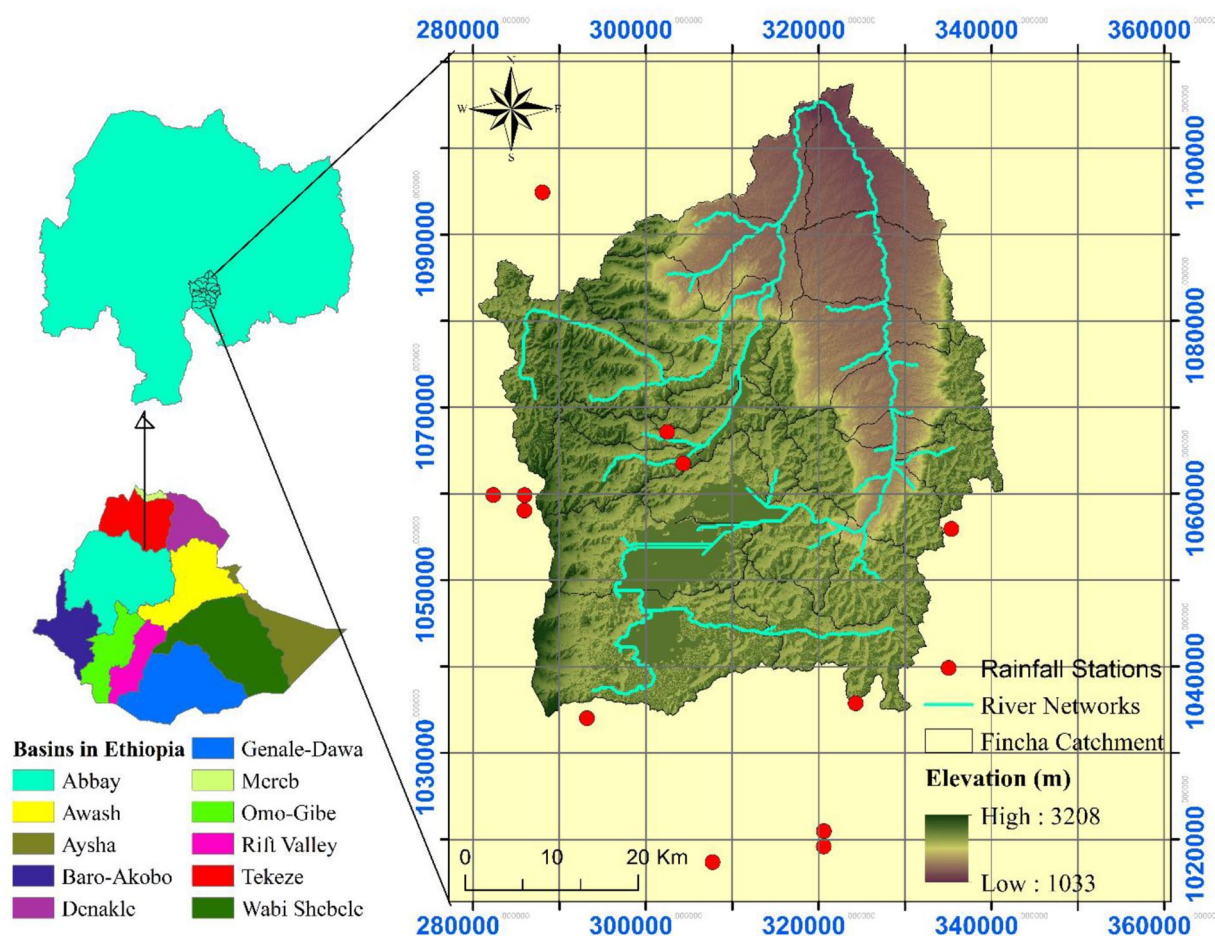


**Figure 1.** Detailed geographic location of the study area.

the delineation of groundwater potential zones is mainly focused on the remotely sensed data available online (Das, 2019; Phinzi & Ngetar, 2019). The accuracy of these data is relatively low when compared to the ground surveyed data (Arefayne Shishaye & Abdi, 2015). The uncertainty in the remote sensing data will propagate throughout the data analysis and will disturb the result (Chang et al., 2007). The influence of the individual criterion was ranked and weighted in Artificial Neural Networks (ANN) training model and Analytical Hierarchy Process (AHP). The correctness of the weights fixed in the ANN and AHP was evaluated with target data assigned to the networks and consistency index (CI) respectively. The weighted overlay analysis in the GIS environment was implemented to generate the promising zones in both approaches (ANN and GIS).

## Method and Materials

### *Description of the study area*

The performance of AI in geospatial analysis and GIS technique for prospecting of potential groundwater promising zones was evaluated in the Fincha catchment, which is found in Abay River Basin, Ethiopia. Fincha river is one of the tributaries of the Abay River. For this specific study, based on the

hydrologic and topographic conditions of this catchment, the place where the Fincha river joins Abay river is considered as the outlet point of the entire regions in the catchment. After fixing the outlet at the junction, all contributing streams (aqua) and watersheds (black) were delineated in the GIS platform as shown in Figure 1. The catchment is geographically located between 37°00'00"E to 37°33'18"E longitude and 09°21'11"N to 10°01'00"N latitude. The meteorological (recorded precipitation) stations contributing to the outlet were identified using Thiessen Polygon. Accordingly, the contributing stations namely: *Alibo*, *Shambu*, *haro*, *Neshi*, *Homi*, *Hareto*, *Gabate*, *Kombolcha*, and *Wayu* were identified. Since the intensity of rainfall and the infiltration capacity of the soil, geologic, and hydrogeologic settings are the main causes for groundwater recharge, the exploration of potential zones considers the rainfall stations. As estimated in the attribute of the delineated catchment, the Fincha river drains a total of 82.11 km<sup>2</sup> areas.

### *GIS-based geospatial analysis for groundwater delineation*

Since the inventory of Global Positioning System (GPS), researchers have been searching for sophisticated software for geospatial analysis (El-Magd et al., 2010; Rajaveni et al., 2017;

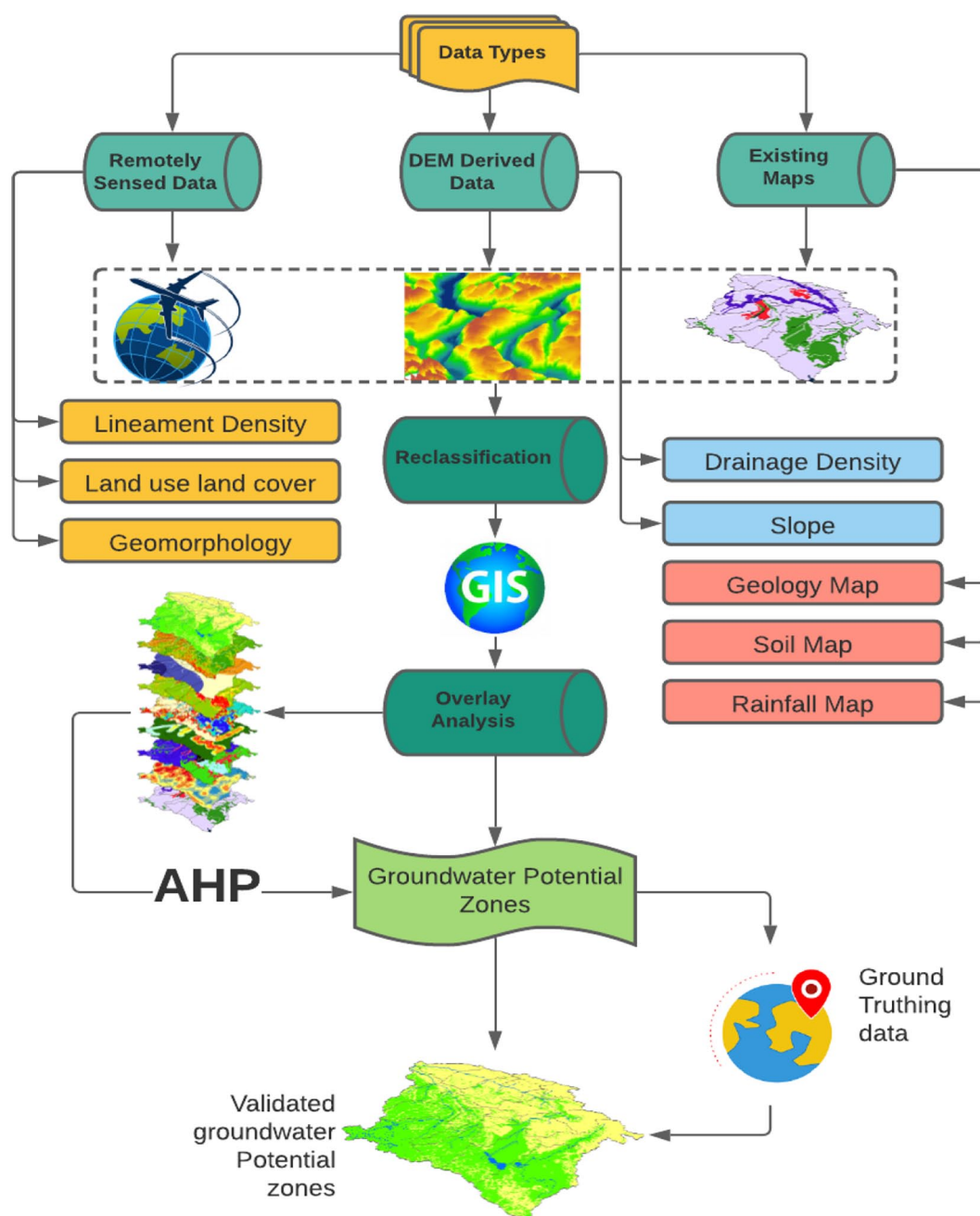


**Figure 2.** Geospatial analysis in GIS and RS for the prospecting of groundwater promising zones.

Singh & Panda, 2017). Geographical Information Systems (GIS) is a computer-based geospatial analysis tool in which an algorithm of the earth's features was built for mapping and analyzing different spatial modeling (Phinzi & Ngetar, 2019). The reason behind the popularity of GIS and RS technology is that due to the difficulties in costs for direct field investigation for data collection (Kayet et al., 2018). The field-based investigation of groundwater requires huge money and takes time to delineate the potential zones. Therefore, the application of GIS and Remote sensing is an effective tool that can save cost and time during the development of a water resource. The exploration of groundwater potential zones in GIS and RS relies on the surface and subsurface significant factors such as slope,

geology, rainfall, geomorphological units, lineament density, lithology, and soil (Berhanu & Hatiye, 2020). GIS and RS is the best tool for the country with limited financial affordability. Ethiopia is known for its sufficient water resources, but the majority of the community is still demanding for daily consumption (Gedam & Dagalo, 2020). Therefore, the aquifer is the primary factor that determines the degree of occurrence of groundwater in a given watershed. The potential zones identifying factors such as rainfall, LULC, lineament density, drainage density, geology, slope, soil, and geomorphologic units used in this study are shown in Figure 2.

The influences of the individual criteria depend on the characteristics of the catchment. As stated in past studies, rainfall,



drainage density, and lineament density reveal the high significance of the occurrence of potential zones when relatively compared with other driving factors. However, the driving factors such as LULLC, slope, soil, geology, drainage density, and lineament density derived from Remote sensing are the major indicators of groundwater potential zones as explained in (Berhanu & Hatiye, 2020). The integration of these significant factors is ranked and weighted in AHP and a thematic map is generated from these weights based on overlay analysis. The Analytical Hierarchy Process (AHP) principle was applied to assign weights through the AHP scale and judgment (Arefayne Shishaye & Abdi, 2015). Then, setting up priorities between the elements to be compared based on the scale, pair-wise comparison matrix for scale consists of the relative importance of the criterion from 1 (equal importance) to 9 (extreme preference of one factor over the other) was applied (Table 1).

The consistency of the weights derived from the pair-wise matrix should be checked and this improves the accuracy of the decision to be made in AHP method. The consistency of the derived values of weights is checked by reducing the error in the estimation and this can be achieved by the method called Consistency Index (CI) and Consistency Ratio (CR) as shown in equations (1) and (2).

$$\text{Consistency Index (CI)} = \frac{\lambda_{\max} - n}{n - 1} \quad (1)$$

$$\text{Consistency Ratio (CR)} = \frac{CI}{RI} \quad (2)$$

Where,  $\lambda_{\max}$  is the maximum Eigen value of the pair-wise matrix,  $n$  is the number of criteria used in the pairwise comparison,  $RI$  is a random Index for a number of an attributes used in the evaluation (Table 2). The  $CR > 0.1$  indicates the correctness of weights assigned in AHP.

**Table 1.** Analytical Hierarchy Process Scale and Judgment.

SCALE	JUDGMENT
1	Equal importance
3	Moderate importance one over the over
5	Essential or strong importance
7	Very strong or demonstrated importance
9	Extreme or absolute importance
2, 4, 6, 8	Intermediate values between the two adjacent judgments

**Table 2.** RI and Attributes.

ATTRIBUTES	3	4	5	6	7	8	9	10
RI	0.52	0.89	1.11	1.25	1.35	1.4	1.45	1.49

### Data-driven (ANN) model

It is a current issue that Artificial Neural Network (ANN) is being used as a powerful tool for water resources management, utilization, and modeling (Dtissibe et al., 2020). A neural network is a data-driven model that focuses on an information processing algorithm to solve a non-linear problem (Lohani et al., 2012). The application of ANN in water resources are getting attention due to its effectiveness (Aichouri et al., 2015). ANN is a data-driven model that is a widely used tool in areas of water resources development and management (Chan & Chan, 2020; Moreno et al., 2020). The selection of an appropriate tool for the delineation of groundwater potential zones depends on the availability of inputs and the skill of how to model the watershed (Lohani et al., 2012). This study evaluates the performance of a data-driven model (ANN) and GIS platforms for the delineation of groundwater potential zones in Fincha catchment. The steps and the input parameters used for the delineation of groundwater potential zones in the ANN model and GIS platform are conceptualized as shown in Figure 3.

The input parameters were distributed over a spatial resolution of  $12.5 \text{ m} \times 12.5 \text{ m}$  before using in the training processes. The productive and non-functional well locations were used as target data while training the ANN model. A multi-layer perceptron (MLP) structure was selected in this study. Based on the number of input parameters assigned in input nodes, which is eight (8), a total of four (4) hidden nodes, and one (1) were used in the hidden layer, and output layer respectively. To start the training processes, the inputs values were normalized using (equation (3)) and random values of weights were assigned. The weight values assigned in the input nodes were multiplied with the normalized and spatially distributed input parameters. The weighted sum of the inputs and weights were activated in hidden nodes using (equation (4)).

$$\text{Normalization} = \frac{X - X_{\min}}{X_{\max} - X_{\min}} \quad (3)$$

$$\text{Activation function} = \frac{1}{1 + e^x} \quad (4)$$

Where  $X$  is the pixel value in the vector point data,  $X_{\min}$  and  $X_{\max}$  the minimum and maximum values in the point-based point values.

**Training ANN model.** Feedforward is the process by which the one-sided sum of weights and inputs parameters are pushed forward to get a rough result in the output node. The difference (error) between the rough result and the target value is very

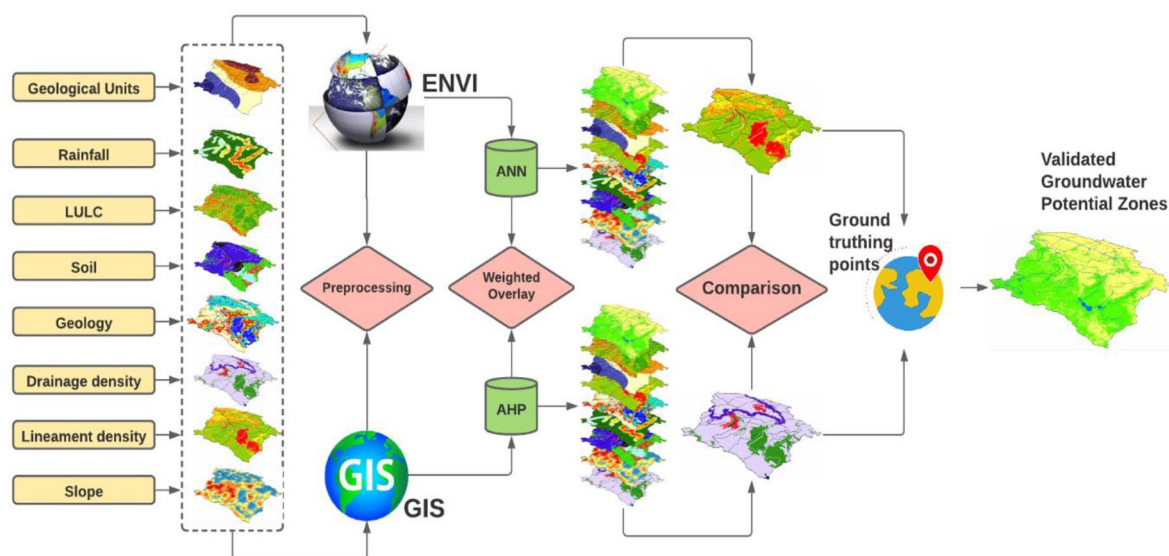


**Figure 3.** Data-driven (ANN) and GIS for the exploration of groundwater potential zones.

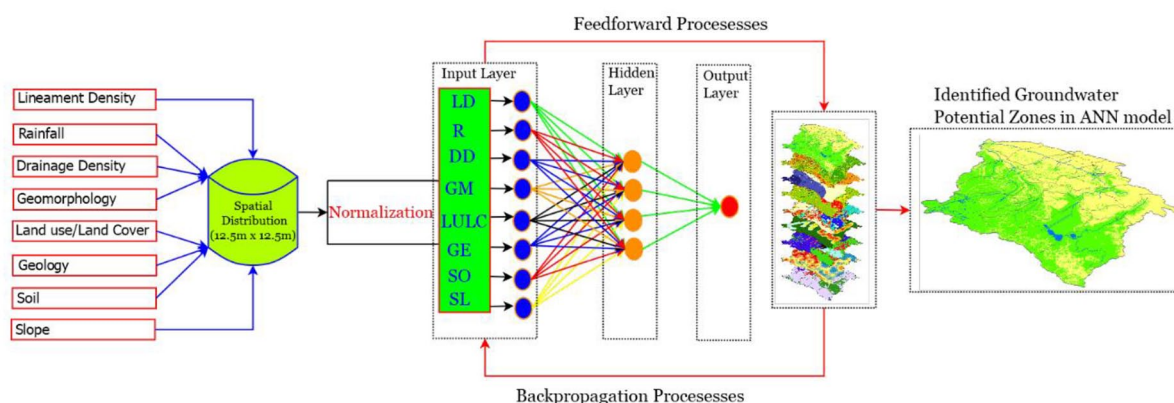


**Figure 4.** Steps of ANN model for prospecting of groundwater potential zones.

Note. LD=lineament density; R=rainfall; DD=drainage density; GM=geomorphology; LULC=land use/land cover; GE=geology; SO=soil; SL=slope.

high at this stage, because, this is the first step of the training process. The reason why the error is high at this level is due to the randomness of the assigned weights. A backpropagation process is a mechanism by which the error between the result and target value is minimized. The overall error obtained at the output layer starts to propagate back into the networks from the output node to the entire network. This process is repeated until an acceptable agreement is made between the model result and target value. The steps used to delineate the potential groundwater zones using the ANN model for this specific study is presented in Figure 4.

### Groundwater Potential Index (GPI)

The occurrence of the Groundwater potential zone is a function of the aquifer characteristics and its spatial extent. The significance of the individual factor in indicating the groundwater potential zones is indexed (Arulbalaji et al., 2019). The criteria selected for the delineation of potential groundwater zones in this catchment were ranked and indexed. The

integration of all the key factors of the groundwater occurrence and movement is computed as GPI (Ahmad, Dar, Teka, et al., 2020). GPI is a unitless parameter used to index (equation (5)) the probability of occurrence of groundwater potential zones in a given catchment. This index provides information about the quantitative-based groundwater classifications as good, moderate, and poor zones. The GPI was generated by weighted overlay analysis using the weight values fixed in ANN and AHP approaches.

$$GPI = \sum_{j=1}^m \sum_{i=1}^n (W_j * X_i) \quad (5)$$

$W_j$ —normalized weight in  $j$  layer, and  $X_i$ —rate value of each class with respect to  $j$  layer.

### Validation

The accuracy of the potential zones delineated in both methods (ANN and GIS technique) was evaluated based on the

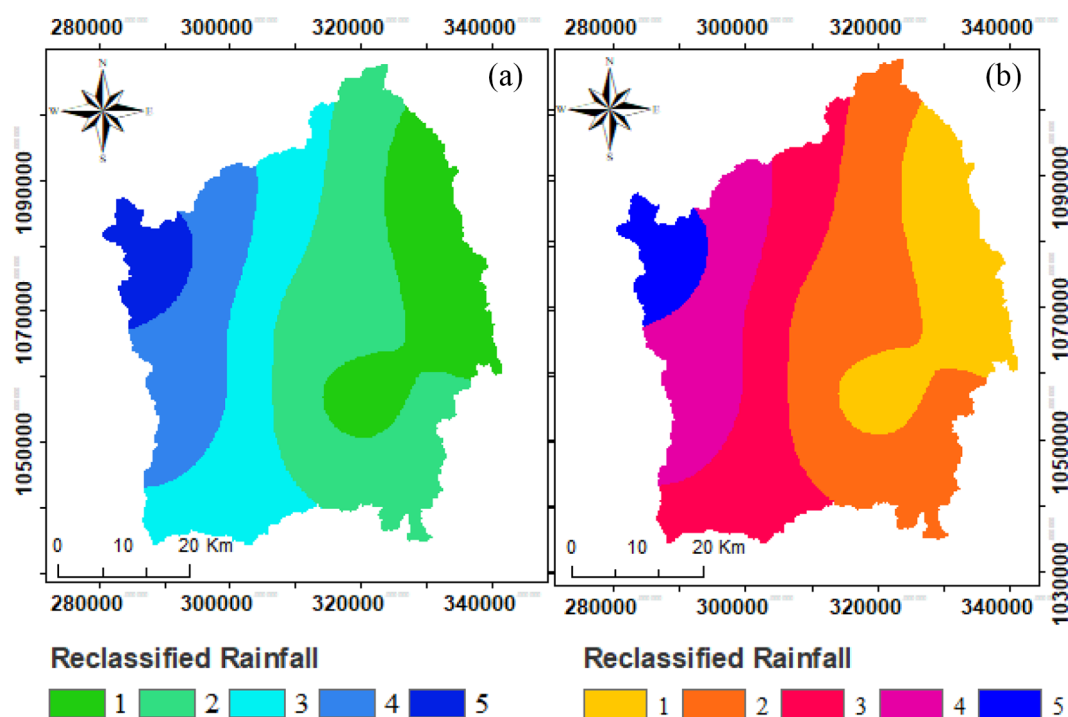


**Figure 5.** Reclassified rainfall thematic maps: (a) GIS tools and (b) ANN model.

potential wells in the study area. A total number of 51 well locations were collected from the local government office and out of this, only 36 well have potential yield and the rest are dried. The pumping rate of the potential well was collected. Since the prediction of the potential zones is the probability, it is required to evaluate the accuracy of the identified zones based on ground-truthing points. The receiver operating characteristics (ROC) curve was used to evaluate the accuracy of the identified groundwater potential zones (Kumar & Krishna, 2018).

## Result and Discussions

The thematic maps generated in the data-driven model and GIS technique for the selected groundwater prospecting criteria (rainfall, LULC, drainage density, lineament density, slope, geology, soil, and Geomorphology) were presented in Figures 5 to 12 respectively. As we can see from these maps, the thematic layers generated in GIS tools were labeled as (a), whereas the results in the data-driven (ANN) model were labeled as (b) in each map. The individual criteria were reclassified based on their importance in indicating the groundwater potential zones. The detailed information about the individual criteria was briefed in the next sections.

### Rainfall

The main source of groundwater recharge is rainfall. A permeable soil that receives rainfall of high intensity can contribute to high groundwater recharge (Ahmad, Dar, Andualem, et al., 2020). The volume of the water stored in an aquifer is a

function of the rainfall intensity and the duration. Water is only stored in the aquifer if the soil and geologic units can transmit it. The rechargeability of groundwater depends on the void spaces in the soil, geologic structures, and the topographic conditions of the area. If the rainfall retains for a long time and the soil is permeable, there is a high probability to recharge groundwater. For potential and permeable aquifers, much amount of water is stored when the rain reached the water table. As shown in Figure 5, the result of reclassified rainfall maps generated in the ANN model and GIS platform were shown in Figure 5a and b respectively. The classifications of the rainfall of the thematic maps in both approaches revealed almost the same categories. This indicates that the ANN model can also be used as an alternative in generating a thematic map. The rainfall was reclassified as very poor=1 (1,548.75–1,617.56 mm), poor=2 (617.56–1,688.70 mm), moderate=3 (1,688.70–1,762.24 mm), high=4 (1,762.24–1,834.04 mm), and very high=5 (1,834.04–1,914.07 mm).

Though there is no study available before the current study regarding the quality and quantity of the groundwater in this catchment, it is evidenced from the community that the main problem is the quantity.

### Land use/land cover

Groundwater recharge is the main process through which the rainfall percolates into an aquifer. This process is a function of land use and land cover. Urbanization is increasing in the catchment and the rechargeability of the groundwater is increasing when compared to the past

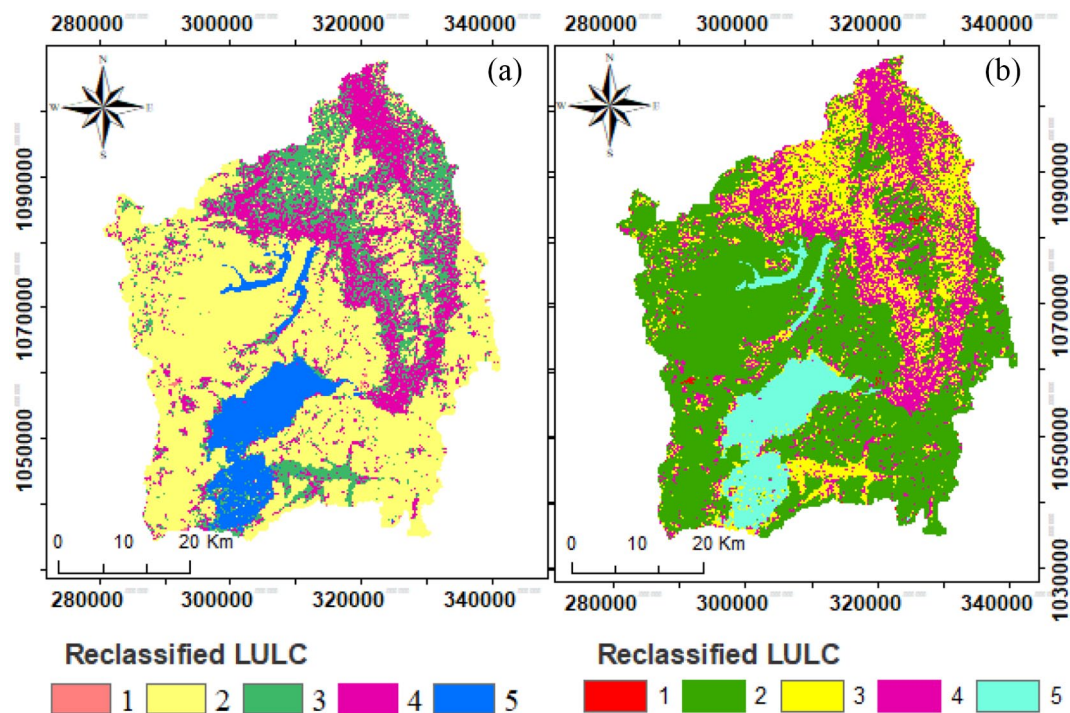


Figure 6. Reclassified land use/land cover thematic maps: (a) GIS tools and (b) ANN model.

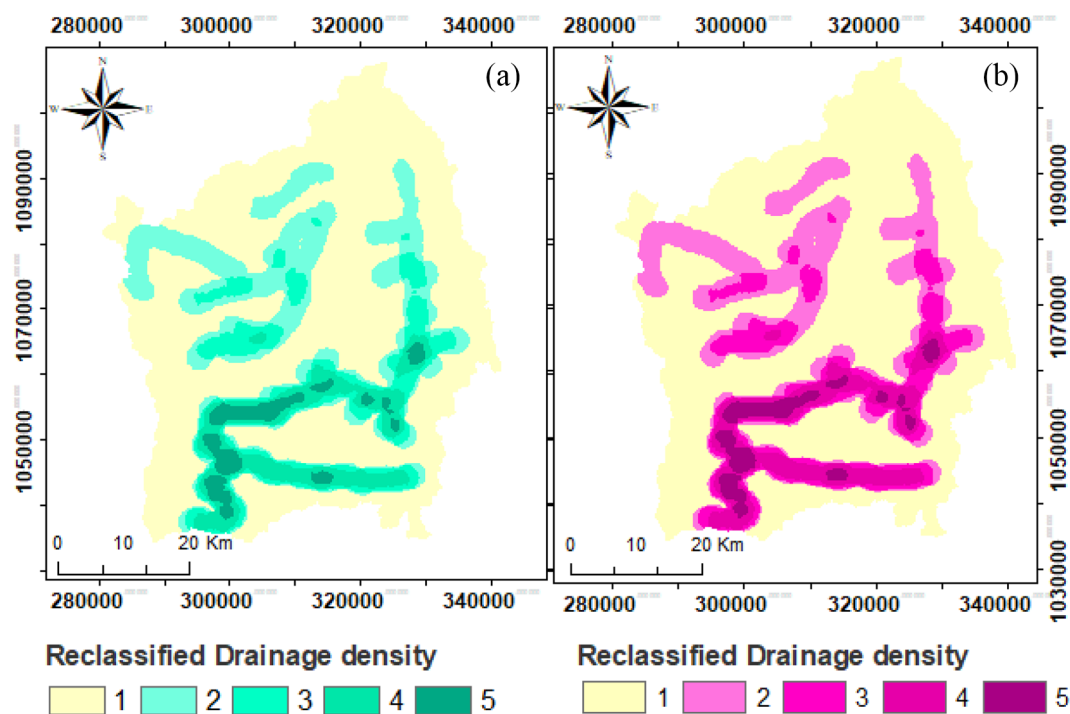


Figure 7. Reclassified drainage density: (a) GIS tools and (b) ANN model.

non-urbanized areas (Hamed et al., 2018). The reclassified LULC thematic maps generated in the ANN model and GIS technique were presented in Figure 6a and b. Five dominant land uses/land covers namely: trees cover areas, shrub cover areas, grassland, cropland, and swampy areas are available in the study area. These were reclassified based on qualitative categories as very poor = 1, poor = 2,

moderate = 3, high = 4, and very high = 5 based on the rate of groundwater recharge.

*Drainage density*

The permeability and the percolation rate of rainfall in specific areas are controlled by the drainage density. Stream networks



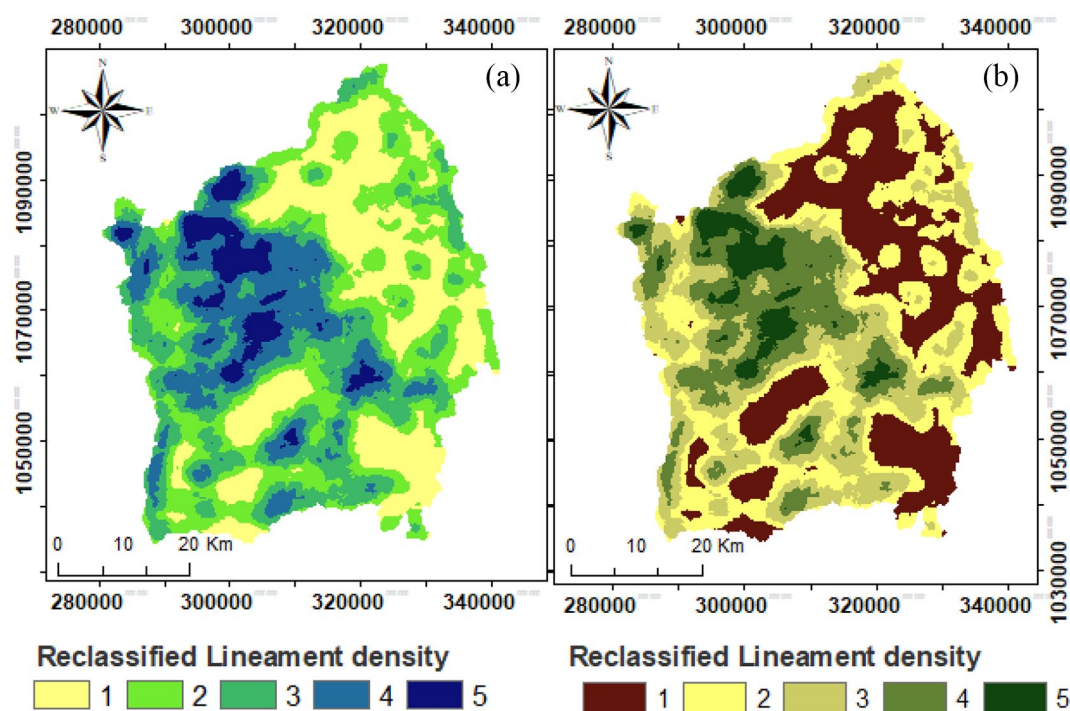


**Figure 8.** Reclassified lineament density thematic maps: (a) GIS tools and (b) ANN model.

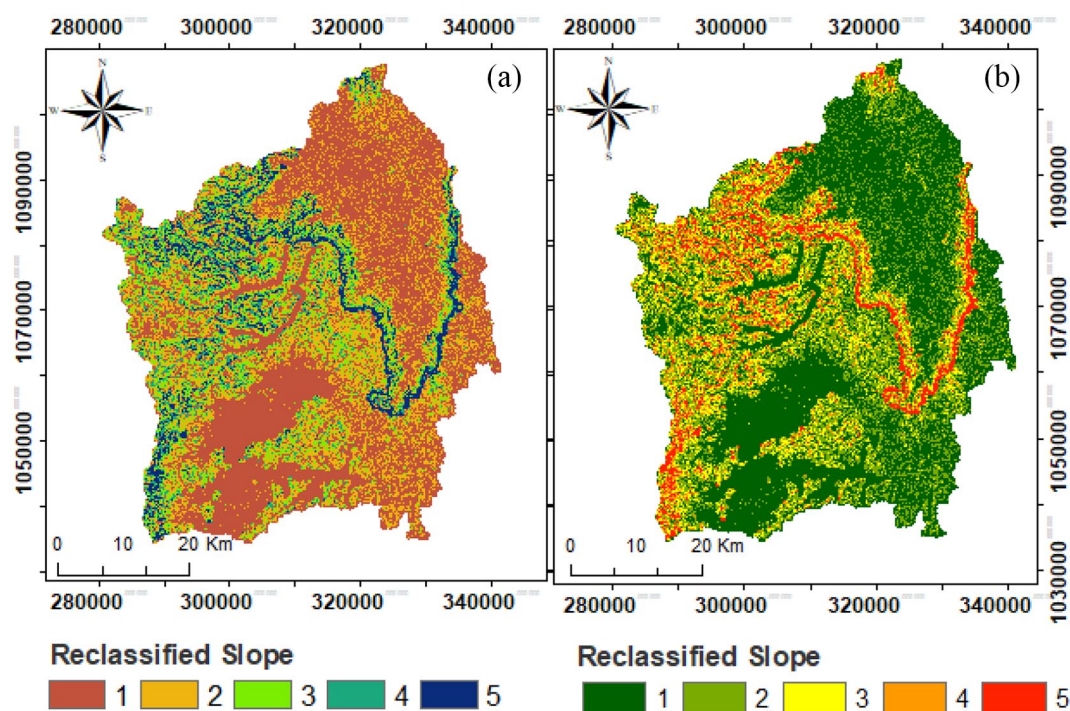


**Figure 9.** Reclassified slope thematic maps: (a) GIS tools and (b) ANN model.

and the corresponding land surface drained across the length of the channel can indicate the potential groundwater zones. The aquifer is potential if the drainage density in the catchment is contributing to groundwater recharge. The hydrogeologic conditions and moisture-holding capacity of the soil initiates the drainage density and this, in turn, support the rechargeability of the groundwater. Drainage density is influenced by the

topographic conditions and the permeability of the geologic units. If the slope is flat, the permeability is very high and the drainage density is very low. Drainage density derived from Digital Elevation Model (DEM) was classified as very poor = 1 (6.58–11.70 km/km<sup>2</sup>), poor = 2 (11.70–17.70 km/km<sup>2</sup>), moderate = 3 (17.70–24.30 km/km<sup>2</sup>), high = 4 (24.30–32.50 km/km<sup>2</sup>), and very high = 5 (32.50–46.60 km/km<sup>2</sup>). The reclassified

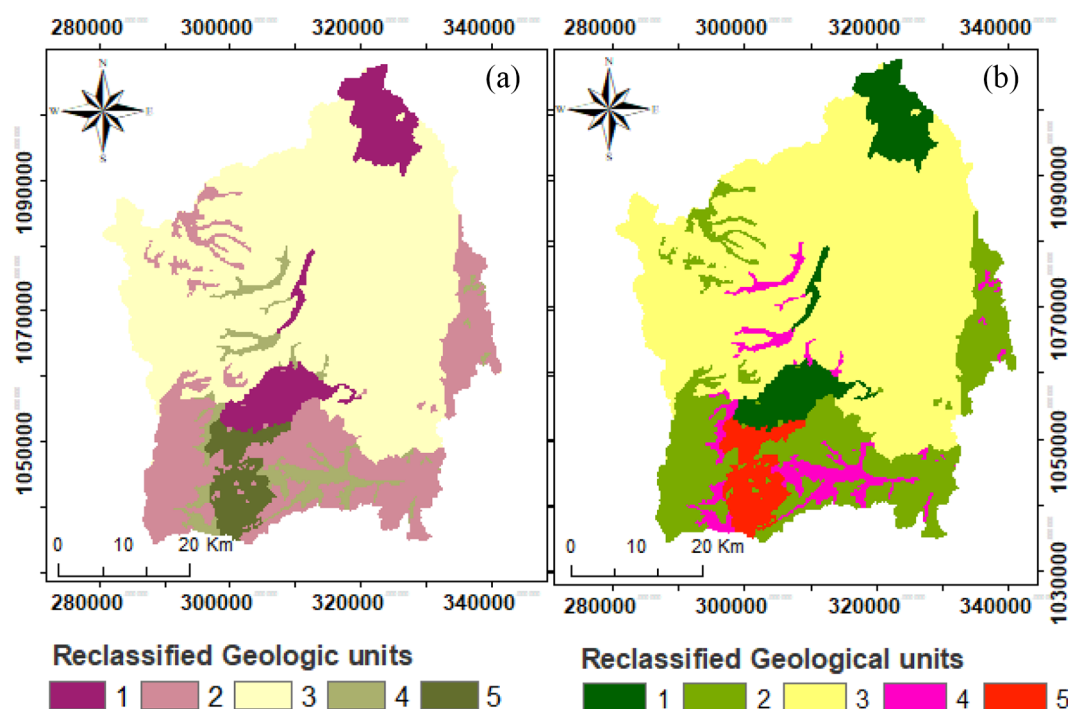


**Figure 10.** Reclassified geologic thematic maps: (a) GIS tools and (b) ANN model.

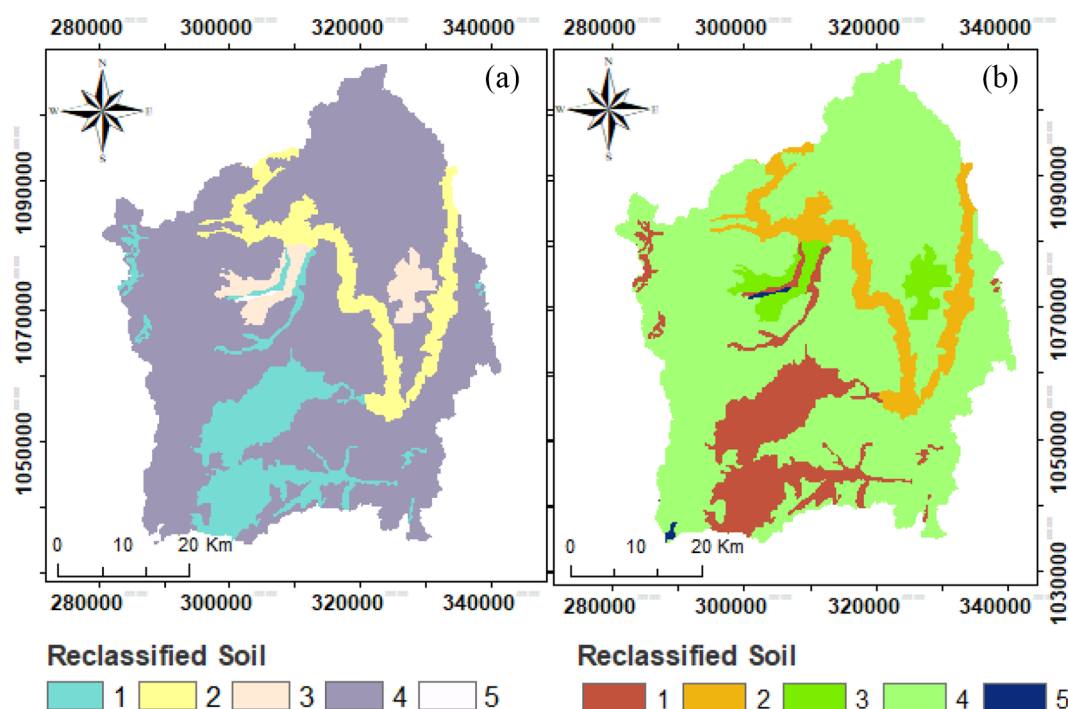


**Figure 11.** Reclassified soil thematic maps: (a) GIS tools and (b) ANN model.

drainage density of the thematic maps generated in the ANN model and GIS technique was presented in Figure 7a and b.

### Lineament density

The features of the lineament of a watershed provide important evidence about the hydrogeology of a given catchment. The features of the lineament density derived from LANDSAT

8 imageries supported by the ground-truthing points can provide information about the status of groundwater rechargeability. Studies conducted in Berhanu and Hatiye (2020), Fenta et al. (2015), and Kapilan and Elangovan (2018) confirmed the importance of lineament density in providing information about the rechargeability of the hydrogeologic settings of a catchment. Lineaments are linear lines and zones of localized weathering that increase the permeability and porosity in the

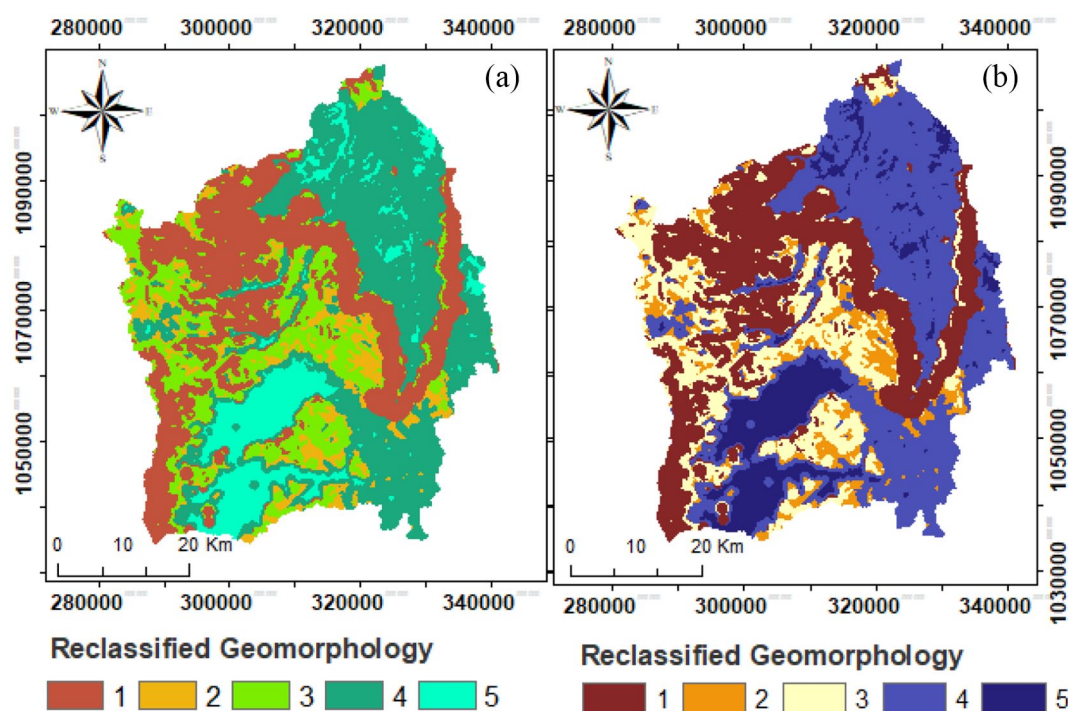


**Figure 12.** Reclassified geomorphologic units thematic maps: (a) GIS tools and (b) ANN model.

geologic settings. The lineament density derived from LANDSAT 8 imageries was classified as very poor = 1 (0.441–0.685 km/km<sup>2</sup>), poor = 2 (0.685–0.938 km/km<sup>2</sup>), moderate = 3 (0.938–1.200 km/km<sup>2</sup>), high = 4 (1.20–1.530 km/km<sup>2</sup>), very high = 5 (1.530–2.390 km/km<sup>2</sup>). The thematic maps of the lineament density generated both in GIS tools and the ANN model were presented in Figure 8a and b respectively.

### Slope

The slope is one of the key significant factors and important in identifying the groundwater recharge zones in a given catchment. The basic concept behind the importance of slope in groundwater recharge is the retention period. The speed, and retention time of surface runoff, and the infiltration capacity of the geologic units are influenced by the slope. The flat regions in the catchment are good indicators of groundwater potential zones as the retention time and infiltration rate are high. The majority of lower portions of the catchment are categorized under steep slopes and the groundwater potential zone ranges from very low to low. The speed of the surface runoff is very high and the retention period are very low due to the steepness of the topography. When the slope is flat enough, the surface runoff gets much time to percolate into the subsurface. For this study, the slopes were reclassified into five categories to groundwater potential zones as very high = 5 (6.59%–11.30%), high = 4 (11.30%–16.6%), moderate = 3 (16.60%–23.20%), poor = 4 (23.2%–32.1%), and very poor = 5 (32.1%–45.8%) as shown in Figure 9a and b.

### Geology

The existence of groundwater in an aquifer depends on the nature of the geology and permeability of the geologic settings. Water is stored in the aquifer when the geologic formation holds and conveys the percolating water. The amount and volume of water stored in the geology is a function of the hydrogeologic settings of the area. The water can only be stored if sufficient void spaces are there between the geologic units. The aquifer is assumed to be potential when there are enough spaces in the hydrogeologic settings. The geologic units with uniform grain size usually have sufficient porosity and high permeability. Groundwater recharge occurs from precipitation that percolates into the subsurface from the surface runoff, lakes, and streams. Fincha river and Fincha lake are permeable and allow the seepage of surface water into the subsurface. The dominant geologic classes of the study area are grouped into Adigrate Sandstone, Blue Nile basalts, Alluvium, colluvium, and marsh soils, and the corresponding classes to the groundwater potential zones are very poor = 1, poor = 2, moderate = 3, high = 4, and very high = 5 respectively. The reclassified geologic units in the ANN and GIS platform based on their importance for the delineation of groundwater potential zones are presented in Figure 10a and b.

### Soil

The subsurface water is stored in void spaces between the soil particles. The volume of water stored in the given hydrologic units depends on the texture and size of the soil particles. The



existing soil data obtained from the Ministry of Water, Mineral, and Energy (MWME) was reclassified as a thematic layer in the ANN and GIS platform as shown in Figure 11a and b respectively. Reclassification was made based on the permeability and infiltration capacity of the soil. However, according to the information obtained from productive wells, the depths are deep and for such cases, the effect of soil is relatively low. Therefore, other factors such as rainfall, LULC, and drainage density played a great role in recharging and contributing to the sub-surface water. The percolation of rainfall through soil is one of the interesting features which in turn helps to reach the water. If there is a high probability of percolating through the soil, it is obvious that much amount of water is stored in the aquifer. For the sub-basin, there is no well-documented information about the aquifer, but as it can be evidenced from the geophysical investigation conducted, it was found that there is high percolation.

### Geomorphology

In the study area, seven dominant landforms namely: flat plains, irregular plains, escarpments, hills, breaks, low mountains, and high mountains. GIS tools and ANN model were used to reclassify the landforms based on their significance of contributing to groundwater. A thematic layer was generated in both methods and the dominant landforms were reclassified into five groups. The landforms of a geomorphologic unit vary in terms of their characteristics and spatial distribution. The occurrence and movement of the subsurface water depend on the geomorphologic characteristics of the area. The low mountainous and flat plains are indicators for the occurrence of groundwater if the hydrogeologic settings transmit water. For a geomorphological unit, a slope-based landform classification was implemented and a quantitative classification namely: very poor=1 (high mountainous), poor=2 (Hills), Moderate=3 (low mountainous), high=4 (breaks), and very high=5 (flat plains) as shown in Figure 12a and b.

The principle of a pair-wise comparison matrix developed in AHP and the overall weights for the evaluated criteria for the delineation of groundwater potential zones in the watershed was summarized in Table 3. The consistency of the AHP technique in capturing the exploration of surface irrigation potential zones is evaluated by consistency Index (CI) and Consistency Ratio (CR) and the summary of this consistency evaluation is as presented in Table 3. As we can see from the table, the  $CI < 0.1$ , and indicates that the values of weight assigned for the individual key factor in AHP are correct. The final updated weights were initially assigned between the input nodes and the hidden nodes, and between hidden nodes and the output node. The result of updated weights after backpropagation processes were re-assigned in the ANN model during the testing periods. The updated weights in the ANN model were taken after the training processes were reached. The

productive wells, pumping data, and other ground-truthing data such as the location of spring and hand-dug well locations collected by hand GPS were used as the target data, and the delineation of the groundwater potential was repeatedly evaluated until an agreement was made between the target and the model result. Since there are eight (8) nodes in the input layer, four (4) nodes in the hidden layer, and one (1) node in the output layer; a total of 38 synoptic connections (weights) are there in the neural networks (NN) selected for this specific study. The values of weights taken after the training processes. The updated values of weight used in the weighted overlay analysis for each criterion were fixed as 0.35, 0.19, 0.27, 0.28, 0.07, 0.31, and 0.06 for lineament density, LULC, slope, drainage density, soil, geology, and geomorphology respectively.

### Delineation of groundwater potential zones (GPZ)

The values of weights fixed in ANN and AHP were used to index groundwater potential zones. Weights fixed in the training processes and AHP were assigned to the corresponding key factors (lineament density, LULC, slope, drainage density, soil, geology, and geomorphology) to generate the groundwater potential zones. Weighted overlay analysis tool in the GIS platform was used in both methods. The delineated Groundwater Potential zones using the GIS platform and ANN model were presented in Figures 13 and 14. As we can see from Figure 13, delineated potential zones were only classified into four qualitative-based classifications as High, Moderate, Low, and Very low, whereas, in Figure 14, five groundwater potential zones were identified including very good qualitative classification. The probability of getting groundwater potential zones with five classifications was obtained in the ANN model, whereas four classifications were obtained in the GIS platform.

### Validation of the potential zones

The accuracy of the delineated groundwater potential zones further evaluated with existing water sources (Berhanu & Hatiye, 2020; Das & Pardeshi, 2018; Duan et al., 2016). The total number of 51 well locations were collected from the local government office and out of this, only 36 well have potential yield and the rest are dried. The pumping rate of the potential well were collected. Since the prediction of the potential zones is probability, it mandatory to evaluate the accuracy of the identified zones based on ground-truthing points. As we can see from the validated potential zones presented in Figures 13 and 14, the majority of existing water sources such as shallow and hand-dug wells are almost overlapped up to 86% and 82.5% with the delineated potential zones in ANN model and GIS technique respectively. The accuracy of the predicted the potential zones evaluated in ROC curve also witness the agreement made between the identified potential zones and the



**Table 3.** Pair-Wise Comparison Matrix of the Key Factors.

	LD	DD	SL	LULC	R	SO	GE	GM	
LD	1.00	3.00	0.25	5.00	2.00	0.33	0.17	3.00	
DD	0.33	1.00	0.50	0.33	5.00	4.00	0.13	4.00	
SL	4.00	2.00	1.00	2.00	0.25	0.33	0.33	0.20	
LULC	0.20	3.00	0.50	1.00	0.33	0.50	2.00	3.00	
R	0.50	0.20	4.00	3.00	1.00	3.00	5.00	0.14	
SO	0.08	0.19	0.07	0.21	0.38	1.00	0.19	0.03	
GE	6.00	8.00	3.00	0.50	0.20	0.33	1.00	0.25	
GM	0.33	0.25	5.00	0.33	7.00	0.20	4.00	1.00	
Col. total	17.37	17.78	14.50	12.29	18.78	15.01	14.63	17.59	
Normalized pair-wise comparison matrix									
LD	0.06	0.17	0.02	0.41	0.11	0.07	0.01	0.17	0.01
DD	0.02	0.06	0.03	0.03	0.27	0.15	0.01	0.23	0.17
SL	0.23	0.11	0.07	0.16	0.01	0.31	0.02	0.01	0.23
LULC	0.01	0.17	0.03	0.08	0.02	0.47	0.14	0.17	0.47
R	0.03	0.01	0.28	0.24	0.05	0.35	0.34	0.01	0.02
SO	0.08	0.19	0.07	0.21	0.38	0.23	0.04	0.19	0.03
GE	0.35	0.45	0.21	0.04	0.01	0.01	0.07	0.01	0.03
GM	0.02	0.01	0.34	0.03	0.37	0.14	0.27	0.06	0.01
NORMALIZED SUM OF ROWS				NORMALIZED AVERAGE ROWS			EIGEN VECTOR		
LD	0.95			0.95/9			0.12		
DD	0.81			0.81/9			0.10		
SL	0.85			0.85/9			0.11		
LULC	1.09			1.09/9			0.13		
R	0.98			0.98/9			0.12		
SO	1.07			1.07/9			0.18		
GE	1.17			1.17/9			0.14		
GM	1.12			1.12/9			0.14		

Note. LD=lineament density; DD=drainage density; SL=slope; LULC=land use/land cover; R=rainfall; SO=soil; GE=geology; GM=geomorphology;  $\lambda=8.125$ ;  $n=8$ ; CI (consistency index)=0.017; RI (random index)=1.4; CR=0.01.

ground-truthing points. The performance of both methods was evaluated in ROC separately. As we can see from the Figures 15 and 16, the area under curve (AUC) of 0.96 and 0.91 were estimated for the ROC curve plotted in the ANN and GIS results respectively. The AUC computed in both methods revealed an agreement of 96% and 91% were made between the ground-truthing points and the ANN model and between GIS platforms respectively. The ROC curve plotted as

the false positive ( $x$ -axis) and true positive rate ( $y$ -axis) was shown in Figure 17.

### Conclusion

The study presents the performance evaluation made between the ANN and GIS platforms for the delineation of groundwater potential zones in Fincha catchment, Abay Basin, Ethiopia. The two methods; data-driven (ANN) model and the GIS

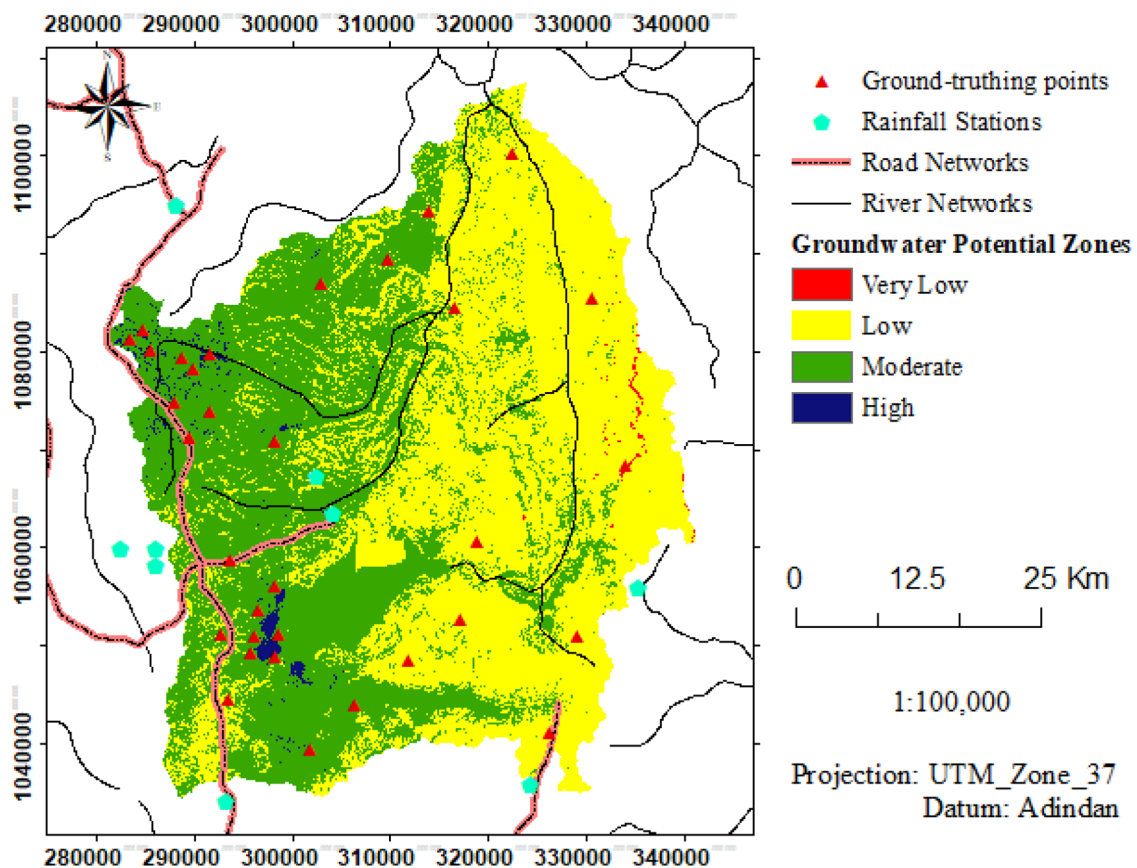


Figure 13. Delineated groundwater potential zones in GIS platforms.

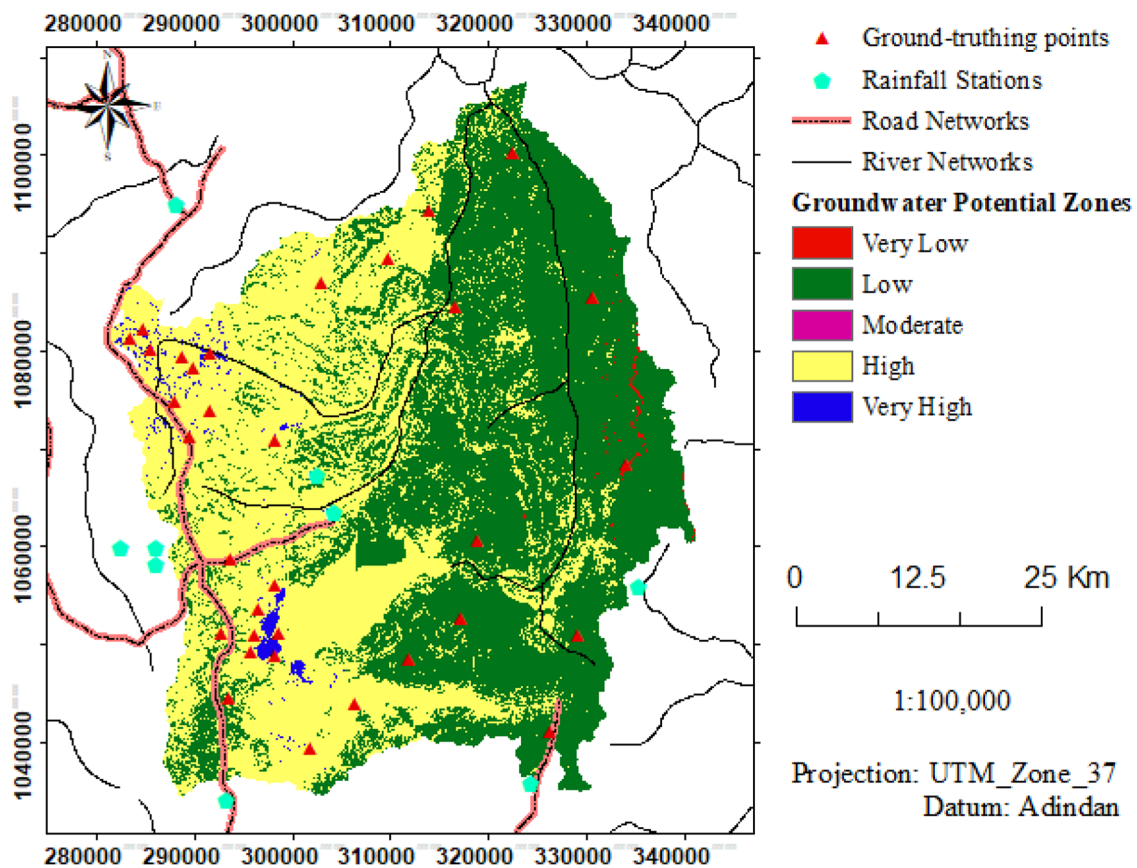
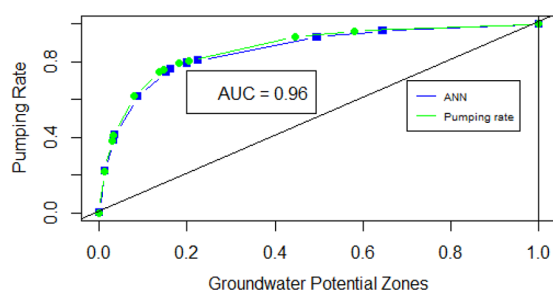
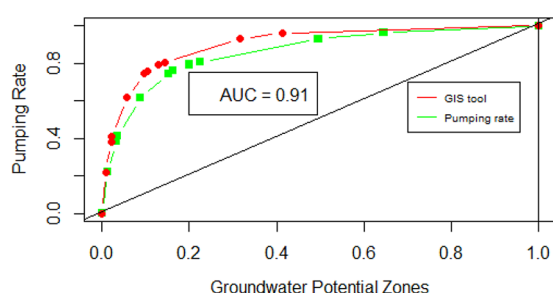


Figure 14. Delineated groundwater potential zones in ANN model.



**Figure 15.** ROC curve for validation of groundwater potential zones delineated in ANN model.



**Figure 16.** ROC curve for validation of groundwater potential zones delineated in ANN model.

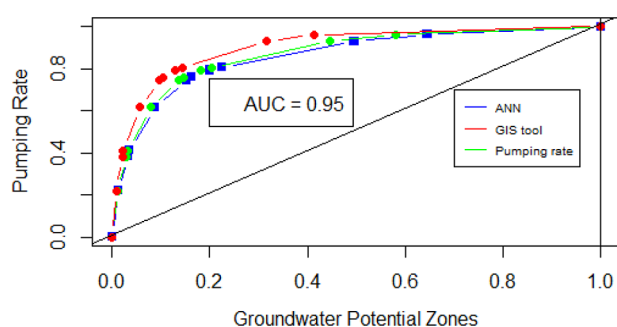


**Figure 17.** ROC curve for comparison of results in ANN model and GIS platforms.

technique were successfully applied to delineate the groundwater potential zones using the key significant factors such as rainfall, slope, LULC, soil, drainage density, lineament density, geology, and Geomorphology as groundwater prospecting criteria. The selected criteria were prepared and distributed on the 12.5 m  $\times$  12.5 m spatial resolution, and normalized before assigning to the neural networks (NN). The importance of the selected criteria was ranked and weighted in ANN and AHP approaches that the training processes and prioritization were implemented in each method respectively. The accuracy of the weights generated in the ANN training model and AHP approach was evaluated by the target values assigned to the networks and Consistency Index (CI) respectively. The thematic map was prepared for the individual criteria and the groundwater potential zones were delineated using the weights fixed in the ANN training model and AHP respectively. Five

and four classes of groundwater potential zones as (Very High, High, Moderate, Low, and Very low) and (High, Moderate, Low, and Very low) were delineated in the ANN and GIS platform respectively. Receiver operating characteristics (ROC) curve developed from pumping rate and ground-truthing points were used to validate the accuracy of the predicted groundwater potential zones. The area under curve (AUC) computed from the ROC curve showed that 96% and 91% agreement were made in the ANN model and GIS platform results respectively. Therefore, the performance of the ANN was better than the GIS technique in delineating the potential zones. Finally, it is concluded that the ANN model is an effective tool for the delineation of groundwater prospective zones, and this paper will recommend that future research will focus on the implementation of the ANN model for the delineation of potential groundwater zones for the region where the cost for direct field investigation is not affordable.

### Authors' Contributions

The correspondent author initiated the research idea, reviewed relevant literature, designed the methods, conducted field data collection, performed data cleaning, analyzed the data, interpretation, and prepare draft manuscripts for publication. Co-authors evaluated and approved the research idea, supervised the whole research activities, and developed the manuscript. All authors read and approved the final manuscript.

### Declaration of Conflicting Interests

The author(s) declared no potential conflicts of interest with respect to the research, authorship, and/or publication of this article.

### Funding

The author(s) received no financial support for the research, authorship, and/or publication of this article.

### ORCID iD

Habtmu Tamiru  <https://orcid.org/0000-0002-2412-6017>

### REFERENCES

- Ahmad I., Dar M. A., Andualem T. G., Tekla A. H., & Tolosa A. T. (2020a). GIS-based multi-criteria evaluation for deciphering of groundwater potential. *Journal of the Indian Society of Remote Sensing*, 48(2), 305–313. <https://doi.org/10.1007/s12524-019-01078-3>
- Ahmad I., Dar M. A., Tekla A. H., Teshome M., Andualem T. G., Teshome A., & Shafi T. (2020b). GIS and fuzzy logic techniques-based demarcation of groundwater potential zones: A case study from Jemma River basin, Ethiopia. *Journal of African Earth Sciences*, 169, 103860. <https://doi.org/10.1016/j.jafrearsci.2020.103860>
- Aichouri I., Hani A., Bougherira N., Djabri L., Chaffai H., & Lallahem S. (2015). River flow model using artificial neural networks. *Energy Procedia*, 74, 1007–1014. <https://doi.org/10.1016/j.egypro.2015.07.832>
- Arefayne Shishaye H., & Abdi S. (2015). Groundwater exploration for water well site locations using geophysical survey methods. *Journal of Waste Water Treatment & Analysis*, 7(1), 1–7. <https://doi.org/10.4172/2157-7587.1000226>
- Arulbalaji P., Padmalal D., & Sreelash K. (2019). GIS and AHP techniques based delineation of groundwater potential zones: A case study from Southern Western Ghats, India. *Scientific Reports*, 9(1), 2082. <https://doi.org/10.1038/s41598-019-38567-x>

- Berhanu K. G., & Hatiye S. D. (2020). Identification of groundwater potential zones using proxy data: Case study of Megech watershed, Ethiopia. *Journal of Hydrology Regional Studies*, 28, 100676. <https://doi.org/10.1016/j.ejrh.2020.100676>
- Chan V. K. H., & Chan C. W. (2020). Towards explicit representation of an artificial neural network model: Comparison of two artificial neural network rule extraction approaches. *Petroleum*, 6(4), 329–339. <https://doi.org/10.1016/j.petlm.2019.11.005>
- Chang F. J., Chiang Y. M., & Chang L. C. (2007). Multi-step-ahead neural networks for flood forecasting. *Hydrological Sciences Journal*, 52(1), 114–130. <https://doi.org/10.1623/hysj.52.1.114>
- Das S. (2019). Geospatial mapping of flood susceptibility and hydro-geomorphic response to the floods in Ulhas basin, India. *Remote Sensing Applications Society and Environment*, 14, 60–74. <https://doi.org/10.1016/j.rsase.2019.02.006>
- Das S., & Pardeshi S. D. (2018). Integration of different influencing factors in GIS to delineate groundwater potential areas using IF and FR techniques: A study of Pravara basin, Maharashtra, India. *Applied Water Science*, 8(7), 1–16. <https://doi.org/10.1007/s13201-018-0848-x>
- Dtissibe F. Y., Ari A. A. A., Titouna C., Thiare O., & Gueroui A. M. (2020). Flood forecasting based on an artificial neural network scheme. *Natural Hazards*, 104(2), 1211–1237. <https://doi.org/10.1007/s11069-020-04211-5>
- Duan H., Deng Z., Deng F., & Wang D. (2016). Assessment of groundwater potential based on multicriteria decision making model and decision tree algorithms. *Mathematical Problems in Engineering*, 2016, 1–11. <https://doi.org/10.1155/2016/2064575>
- El-Magd I. A., Hermas E., & Bastawesy M. E. (2010). GIS-modelling of the spatial variability of flash flood hazard in Abu Dabbab catchment, Red Sea region, Egypt. *The Egyptian Journal of Remote Sensing and Space Science*, 13(1), 81–88. <https://doi.org/10.1016/j.ejrs.2010.07.010>
- Fenta A. A., Kifle A., Gebreyohannes T., & Hailu G. (2015). Spatial analysis of groundwater potential using remote sensing and GIS-based multi-criteria evaluation in Raya Valley, northern Ethiopia. *Hydrogeology Journal*, 23(1), 195–206. <https://doi.org/10.1007/s10040-014-1198-x>
- Hamed Y., Hadji R., Redhaounia B., Zighmi K., Bâali F., & El Gayar A. (2018). Climate impact on surface and groundwater in North Africa: A global synthesis of findings and recommendations. *Euro-Mediterranean Journal for Environmental Integration*, 3(1), 1–15. <https://doi.org/10.1007/s41207-018-0067-8>
- Kapilan S., & Elangovan, K. (2018). Potential landfill site selection for solid waste disposal using GIS and multi-criteria decision analysis (MCDA). *Journal of Central South University*, 25(3), 570–585. <https://doi.org/10.1007/s11771-018-3762-3>
- Kayet N., Pathak K., Chakrabarty A., & Sahoo S. (2018). Evaluation of soil loss estimation using the RUSLE model and SCS-CN method in hillslope mining areas. *International Soil and Water Conservation Research*, 6(1), 31–42. <https://doi.org/10.1016/j.iswcr.2017.11.002>
- Kumar A., & Krishna A. P. (2018). Assessment of groundwater potential zones in coal mining impacted hard-rock terrain of India by integrating geospatial and analytic hierarchy process (AHP) approach. *Geocarto International*, 33(2), 105–129. <https://doi.org/10.1080/10106049.2016.1232314>
- Li P. (2016). Groundwater quality in Western China: Challenges and paths forward for groundwater quality research in Western China. *Exposure and Health*, 8(3), 305–310. <https://doi.org/10.1007/s12403-016-0210-1>
- Lohani A. K., Kumar R., & Singh R. D. (2012). Hydrological time series modeling: A comparison between adaptive neuro-fuzzy, neural network and autoregressive techniques. *Journal of Hydrology*, 442–443, 23–35. <https://doi.org/10.1016/j.jhydrol.2012.03.031>
- Mandal B., Dolui G., & Satpathy S. (2018). Land suitability assessment for potential surface irrigation of river catchment for irrigation development in Kansai watershed, Purulia, West Bengal, India. *Sustainable Water Resources Management*, 4(4), 699–714. <https://doi.org/10.1007/s40899-017-0155-y>
- Moreno J. M., Sánchez J. M., & Espitia H. E. (2020). Use of computational intelligence techniques to predict flooding in places adjacent to the Magdalena river. *Heliyon*, 6(9), e04872. <https://doi.org/10.1016/j.heliyon.2020.e04872>
- Natarajan S., & Radhakrishnan N. (2020). An integrated hydrologic and hydraulic flood modeling study for a medium-sized ungauged urban catchment area: A case study of Tiruchirappalli city using HEC-HMS and HEC-RAS. *Journal of the Institution of Engineers (India) Series A*, 101(2), 381–398. <https://doi.org/10.1007/s40030-019-00427-2>
- Ouma Y. O., Okuku C. O., & Njau E. N. (2020). Use of artificial neural networks and multiple linear regression model for the prediction of dissolved oxygen in rivers: Case study of hydrographic basin of River Nyando, Kenya. *Complexity*, 2020, 1–23. <https://doi.org/10.1155/2020/9570789>
- Pasalari H., Nodehi R. N., Mahvi A. H., Yaghmaeian K., & Charrahi Z. (2019). Landfill site selection using a hybrid system of AHP-fuzzy in GIS environment: A case study in Shiraz city, Iran. *MethodsX*, 6, 1454–1466. <https://doi.org/10.1016/j.mex.2019.06.009>
- Phinzi K., & Ngetar N. S. (2019). The assessment of water-borne erosion at catchment level using GIS-based RUSLE and remote sensing: A review. *International Soil and Water Conservation Research*, 7(1), 27–46. <https://doi.org/10.1016/j.iswcr.2018.12.002>
- Rajaveni S. P., Brindha K., & Elango L. (2017). Geological and geomorphological controls on groundwater occurrence in a hard rock region. *Applied Water Science*, 7(3), 1377–1389. <https://doi.org/10.1007/s13201-015-0327-6>
- Rezaeianzadeh M., Tabari H., Arabi Yazdi A., Isik S., & Kalin L. (2014). Flood flow forecasting using ANN, ANFIS and regression models. *Neural Computing and Applications*, 25(1), 25–37. <https://doi.org/10.1007/s00521-013-1443-6>
- Sarkar D., & Mondal P. (2020). Flood vulnerability mapping using frequency ratio (FR) model: A case study on Kulik river basin, Indo-Bangladesh Barind region. *Applied Water Science*, 10(1), 1–13. <https://doi.org/10.1007/s13201-019-1102-x>
- Singh G., & Panda R. K. (2017). Grid-cell based assessment of soil erosion potential for identification of critical erosion prone areas using USLE, GIS and remote sensing: A case study in the Kapgari watershed, India. *International Soil and Water Conservation Research*, 5(3), 202–211. <https://doi.org/10.1016/j.iswcr.2017.05.006>
- Sun Y., Wendi D., Kim D. E., & Liang S. Y. (2019). Deriving intensity–duration–frequency (IDF) curves using downscaled in situ rainfall assimilated with remote sensing data. *Geoscience Letters*, 6(1), 1–12. <https://doi.org/10.1186/s40562-019-0147-x>
- Thiemig V., Rojas R., Zambrano-Bigiarini M., & De Roo A. (2013). Hydrological evaluation of satellite-based rainfall estimates over the Volta and Baro-Akobo Basin. *Journal of Hydrology*, 499, 324–338. <https://doi.org/10.1016/j.jhydrol.2013.07.012>
- Worqlul A. W., Jeong J., Dile Y. T., Osorio J., Schmitter P., Gerik T., Srinivasan R., & Clark N. (2017). Assessing potential land suitable for surface irrigation using groundwater in Ethiopia. *Applied Geography*, 85, 1–13. <https://doi.org/10.1016/j.apgeog.2017.05.010>